

A MODIFIED TAGUCHI'S OPTIMIZATION ALGORITHM FOR BEAMFORMING APPLICATIONS

Z. D. Zaharis*

Telecommunications Center, Aristotle University of Thessaloniki,
Thessaloniki 54124, Greece

Abstract—The present paper is a study of adaptive beamforming (ABF) techniques applied to antenna arrays. The structure of these techniques is based on Taguchi's Optimization (TagO) method. The high convergence speed and the ability to reach near-optimal solutions by adjusting only one parameter make the Taguchi's method an attractive choice for real time implementations like the case of ABF. Modifications are proposed in order to enhance the applicability of the TagO algorithm and decrease the computational time needed by the algorithm to terminate. The TagO method is used here to construct an ABF technique that aims at steering the main lobe of a uniform linear array towards a signal of interest, under the constraint of low side lobe level (*SLL*) or the constraint of placing radiation pattern nulls towards respective interference signals. Properly defined fitness functions must be minimized by the TagO algorithm to satisfy respectively the above mentioned constraints. The TagO-based ABF technique is compared with typical beamforming methods, like the Sample Matrix Inversion (SMI) and Maximum Likelihood (ML) ones, and with two evolutionary ABF techniques based on Particle Swarm Optimization (PSO) and Differential Evolution (DE), respectively. The comparison is performed regarding the convergence speed, the ability to achieve better fitness values in less time, the ability to properly steer the main lobe and finally the null-steering ability or the *SLL* control depending on the constraint type. The results exhibit the superiority of the TagO-based technique.

Received 1 April 2012, Accepted 5 May 2012, Scheduled 10 May 2012

* Corresponding author: Zaharias D. Zaharis (zaharis@auth.gr).

1. INTRODUCTION

Adaptive beamforming (ABF) is a real time procedure capable of improving the dynamic behavior of an antenna array, which receives signals from directions of arrival (DoA) that change with time [1–19]. Principally, an ABF technique estimates the excitation weights w_m ($m = 1, \dots, M$) that make an M -element array steer the main lobe towards a desired signal called signal of interest (SOI). Such a technique that improves the reception of the SOI in the presence of additive zero-mean Gaussian noise is the Maximum Likelihood (ML) method [20]. Nevertheless, in many cases, the rejection of undesired incoming signals is additionally required by an ABF technique. This requirement is satisfied either by placing radiation pattern nulls towards the respective DoA of the undesired signals or by producing a radiation pattern with low side lobe level (*SLL*). The null-steering can be achieved either by typical ABF methods, such as the Sample Matrix Inversion (SMI) method [20], or by ABF techniques based on evolutionary optimization methods, such as Genetic Algorithms (GAs) [1–3], Particle Swarm Optimization (PSO) [4–9, 11, 13] and Differential Evolution (DE) [14, 15]. Due to its structure, the SMI method does not perform *SLL* control. On the contrary, an evolutionary optimization method has the ability to achieve low *SLL* by minimizing a properly defined fitness function. Therefore, every evolutionary method is potentially capable of performing either null-steering or *SLL* control. The major disadvantage that makes such a method unsuitable for real time applications is the low convergence speed. Thus, an optimization method with high convergence speed would be desirable for ABF applications.

The present work introduces an effective ABF technique based on the recently announced Taguchi's Optimization (TagO) method [21–25]. To the best of the author's knowledge, the TagO method has never been applied before in antenna array beamforming problems. Some modifications are proposed in order to enhance the applicability of the TagO algorithm and decrease the computational time needed by the algorithm to terminate.

The TagO-based ABF technique is applied here to estimate the excitation weights of uniform linear arrays (ULAs) in several cases with alternative requirements and in comparison with other beamforming techniques. In some of these cases, the proposed technique is compared with a PSO-based beamformer, a DE-based beamformer and the SMI method regarding the convergence speed, the ability to steer the main lobe towards a SOI and the ability to place nulls towards respective interference signals. In the rest cases, the proposed technique is

compared with the same PSO-based and DE-based beamformers and also with the ML method regarding the convergence speed, the ability to steer the main lobe towards a SOI and the ability to minimize the *SLL*.

2. TAGUCHI'S OPTIMIZATION METHOD

The TagO algorithm is thoroughly described in [21]. The algorithm is initialized by selecting a suitable fitness function *fit* and a proper orthogonal array OA (*E*, *P*, *L*, *t*), where *E* is the number of runs (or experiments), *P* is the number of parameters (or variables) to be optimized, *L* is the number of *levels*, and finally *t* is the *strength*. An orthogonal array with 3 levels and strength 2, i.e., OA (*E*, *P*, 3, 2), has been found to be efficient for most problems [21–25]. This type of OA is used below.

For each *i*th iteration and each *p*th parameter, the *level difference* LD_{pi} is calculated according to the expression:

$$LD_{pi} = rr^{i-1} \cdot LD_{p1}, \quad p = 1, \dots, P \quad (1)$$

where

$$LD_{p1} = (\max_p - \min_p) / (L + 1), \quad p = 1, \dots, P \quad (2)$$

is the *initial level difference* and *rr* is the *reduced rate*. Also, \max_p and \min_p are respectively the upper and the lower bound of the *p*th parameter. By increasing *rr*, the TagO algorithm usually achieves better results but converges slower. Values of *rr* between 0.75 and 0.90 are good choices for most problems [21, 22, 24]. The value LV_{2pi} of the 2nd level of the *p*th parameter is set equal to the optimum value $opt_{p(i-1)}$ of this parameter derived from the previous iteration (*i*-1), except for the 1st iteration (*i*=1) where $LV_{2p1} = (\max_p + \min_p)/2$. If $opt_{p(i-1)} = \min_p$ then $LV_{2pi} = \min_p + LD_{pi}$, and if $opt_{p(i-1)} = \max_p$ then $LV_{2pi} = \max_p - LD_{pi}$. Afterwards, it is easy to extract the values of the other two levels: $LV_{1pi} = LV_{2pi} - LD_{pi}$ and $LV_{3pi} = LV_{2pi} + LD_{pi}$. At this point, we check LV_{1pi} and LV_{3pi} . So, if $LV_{1pi} < \min_p$ then $LV_{1pi} = \min_p$, and if $LV_{3pi} > \max_p$ then $LV_{3pi} = \max_p$.

Afterwards, the fitness function fit_{ei} is calculated for each experiment *e* (*e* = 1, ..., *E*) and is converted to a negative value in dB according to a logarithmic formula given below:

$$\eta_{ei} = -20 \log fit_{ei}, \quad e = 1, \dots, E \quad (3)$$

The average fitness values in dB are then extracted for each parameter and each level by applying the expression:

$$\bar{\eta}_{lpi} = (L/E) \sum_{e, OA(e,p)=l} \eta_{ei}, \quad p = 1, \dots, P \ \& \ l = 1, 2, 3 \quad (4)$$

In this way, we build the so-called *response table*. The i th iteration terminates with the selection of opt_{pi} . For each p th parameter, opt_{pi} is represented by the value LV_{lpi} that corresponds to the largest value of the set $(\bar{\eta}_{1pi}, \bar{\eta}_{2pi}, \bar{\eta}_{3pi})$. The algorithm terminates at the end of the i th iteration when all ratios LD_{pi}/LD_{p1} ($p = 1, \dots, P$) become less than a converged value, which depends on the desired accuracy.

The above description reveals an important advantage, which makes the TagO algorithm attractive for many applications: that is the ability to affect the performance of the algorithm by adjusting only one parameter, i.e., the reduced rate rr , while other optimization algorithms, like PSO [26–31] and DE [23, 32–34], need to adjust two or more parameters.

2.1. Modified Taguchi's Optimization Algorithm

Due to (3), only positive fitness values are allowed. To enable the TagO algorithm to handle either positive or negative fitness values and thus increase the applicability of the algorithm, these values are not converted to dB but only summed for each parameter and each level. Consequently, the response table is filled only with sums of type

$$\sum_{e, OA(e,p)=l} fit_{ei}$$

without the need either for converting fit_{ei} to dB or for extracting average values. Another difference from the typical TagO algorithm lies in the selection of opt_{pi} . This value is represented by one of $LV_{1pi}, LV_{2pi}, LV_{3pi}$, which corresponds to the minimum sum of fitness values and not to the largest $\bar{\eta}_{lpi}$, as previously defined in the typical TagO algorithm. The absence of logarithmic conversions and average fitness calculations saves computational time and this is an additional advantage obtained from these modifications.

Another modification lies in the termination criterion. The algorithm terminates at the end of the i th iteration when all level differences LD_{pi} ($p = 1, \dots, P$) become less than a desired value. In this way, an optimal solution with the desired accuracy can always be achieved.

3. BEAMFORMING PROBLEM DEFINITION

A ULA consists of M monochromatic isotropic elements, with inter-element distance $q = 0.5\lambda$, and receives a SOI s from angle of arrival (AoA) θ_0 and N interference signals i_n ($n = 1, \dots, N$) from respective AoA θ_n . The SOI is considered as reference signal and therefore its mean power, P_{SOI} , is taken equal to 1 Watt. The interference signals are considered of the same power level as the SOI. Also, the ULA

receives additive zero-mean Gaussian noise signals n_m ($m = 1, \dots, M$) that have the same variance σ^2 , calculated as follows:

$$\sigma^2 = 10^{-SNR/10} \tag{5}$$

where SNR is the signal-to-noise ratio in dB. Each θ_n ($n = 0, 1, \dots, N$) is defined by the DoA of the incoming signal and the normal to the array axis direction. DoA estimation algorithms can be used to calculate the values of θ_n ($n = 0, 1, \dots, N$) [20, 35–40]. Provided that the signals n_m ($m = 1, \dots, M$) are uncorrelated with each other, the noise correlation matrix can be simplified as follows:

$$\bar{R}_{nn} = \sigma^2 I \tag{6}$$

Then, the correlation matrix of the signals x_m ($m = 1, \dots, M$) at the input of the array elements is calculated by the expression:

$$\bar{R}_{xx} = \bar{a}_0 \bar{a}_0^H + \bar{A} \bar{R}_{ii} \bar{A}^H + \sigma^2 I \tag{7}$$

where \bar{R}_{ii} is the interference correlation matrix,

$$\bar{A} = [\bar{a}_1 \quad \bar{a}_2 \quad \dots \quad \bar{a}_N] \tag{8}$$

is the $M \times N$ array steering matrix, and

$$\bar{a}_n = \left[1 \quad e^{j \frac{2\pi}{\lambda} q \sin \theta_n} \quad \dots \quad e^{j(M-1) \frac{2\pi}{\lambda} q \sin \theta_n} \right]^T, \quad n = 0, 1, \dots, N \tag{9}$$

is the array steering vector that corresponds to AoA θ_n .

Depending on the requirements to be satisfied, two beamforming problems can be defined. In the first one, both the main-lobe-steering and null-steering abilities are examined, while in the second, the beamformers are tested regarding both the main-lobe-steering ability and the ability to minimize the *SLL*. The fast convergence of the ABF algorithms is a common requirement for both problems. The formulation of these problems is given below.

3.1. Main-lobe-steering and Null-steering Beamforming Problem

The ABF techniques are tested here regarding the ability to steer the main lobe towards the SOI s and the ability to place nulls towards i_n ($n = 1, \dots, N$). The TagO-based ABF technique is compared with the SMI method and with two ABF techniques based respectively on PSO and DE. The excitation weight calculation using TagO, PSO and DE is achieved by minimizing the following fitness function:

$$F_1(\bar{w}) = k_1 |\theta_0 - \theta_0^{\text{main}}| + k_2 \sum_{n=1}^N \left| \theta_n - \theta_n^{\text{null}} \right| \tag{10}$$

where $\bar{w} = [w_1 \ w_2 \ \dots \ w_M]^T$ is the excitation weight vector, the angle θ_0^{main} indicates the actual direction of the main lobe, the angles θ_n^{null} ($n=1, \dots, N$) indicate the actual directions of the nulls, and finally k_1 and k_2 are minimization balance factors of the two terms given in (10). The SMI method estimates the excitation weights by applying the following expression:

$$\bar{w}_{smi} = \bar{R}_{xx}^{-1} \bar{a}_0 \quad (11)$$

In the examples given below, a 9-element ULA ($M = 9$), with $q = 0.5\lambda$ and $SNR = 10$ dB, is used to confront the above-defined beamforming problem. This problem has 9 unknowns and thus the TagO algorithm makes use of orthogonal array OA (27, 9, 3, 2). Also, the parameter rr is set equal to 0.9 and each execution of the TagO algorithm is completed when $LD_{pi} \leq 0.001$ ($p = 1, \dots, P$).

The PSO algorithm used here is an effective PSO variant called Constriction Factor PSO (CFPSO) [26]. The velocity update parameters, c_1 and c_2 , used by the CFPSO algorithm are set equal to 2.05. Then, the constriction factor K calculated by Equation (6) in [26] is found equal to 0.7298. The maximum velocity V_{max} is limited to the dynamic range of each variable on the respective dimension. Moreover, the CFPSO algorithm makes use of a population size of 27 particles and takes 500 iterations to complete each execution.

Finally, the DE algorithm utilized here is the most popular DE variant and is based on the *DE/rand/1/bin* strategy. The weighting factor F and the crossover constant CR are set respectively equal to 0.5 and 0.9. The DE algorithm makes use of the same population size (27 vectors) and takes the same number of iterations (500 generations) per execution as the CFPSO algorithm.

It must be noted that every experiment in the TagO algorithm has the same meaning as a particle in the CFPSO algorithm or a vector in the DE algorithm. This can be easily understood considering that each experiment or particle or vector corresponds to a fitness function evaluation for every iteration of the algorithm. Given that an orthogonal array of 27 experiments is utilized by the TagO algorithm, the CFPSO and DE algorithms must use a population size of 27 particles or vectors in order to have a fair comparison among the algorithms.

3.2. Main-lobe-steering and SLL-minimization Beamforming Problem

The ABF techniques are tested here regarding the ability to steer the main lobe towards the SOI and the ability to minimize the *SLL*. The

TagO-based ABF technique is compared with the ML method, the PSO-based technique and the DE-based technique. The calculation of \bar{w} using TagO, PSO and DE is achieved by minimizing the fitness function given below:

$$F_2(\bar{w}) = k_1 |\theta_0 - \theta_0^{\text{main}}| + k_2 [\max(SLL, SLL_{des}) - SLL_{des}] \quad (12)$$

where θ_0^{main} , k_1 and k_2 have the same meaning as in (10), and SLL_{des} is the desired SLL value. Due to the second term in (12), SLL values less than SLL_{des} do not cause further minimization of F_2 , since the low SLL requirement has already been satisfied. The ML method estimates \bar{w} as follows:

$$\bar{w}_{ml} = \frac{\bar{R}_{nn}^{-1} \bar{a}_0}{\bar{a}_0^H \bar{R}_{nn}^{-1} \bar{a}_0} \quad (13)$$

In the examples given below, this beamforming problem is solved considering an 11-element ULA ($M = 11$), with $q = 0.5\lambda$ and $SNR = 10$ dB. Thus, the TagO algorithm makes use of OA (27, 11, 3, 2) considering $rr = 0.9$ and terminates when $LD_{pi} \leq 0.001$ ($p = 1, \dots, P$). The CFPSO and DE algorithms are the same as previously described.

4. CONVERGENCE RATE RESULTS

Initially, the TagO-based ABF technique is compared with the PSO-based and DE-based techniques in terms of convergence speed. The convergence speed is a crucial parameter of real time applications like ABF ones. The comparison is performed separately for each one of the above-defined beamforming problems.

4.1. Main-lobe-steering and Null-steering Beamforming Problem

The formulation of the problem and all the parameters concerning the optimization algorithms have already been given in Subsection 3.1. Each one of the TagO-based, PSO-based and DE-based techniques is executed 100 times in order to minimize the fitness function given in (10) and thus extract comparative graphs that display the average convergence rate. The techniques are applied to a 9-element ULA receiving a SOI from AoA $\theta_0 = 30^\circ$ and seven ($N = 7$) interference signals arriving respectively from AoA -70° , -50° , -30° , -10° , 10° , 40° and 60° . The comparative graphs given in Figure 1 show that the TagO-based technique needs fewer iterations to terminate and seems to achieve better fitness values than the other two techniques. Thus,

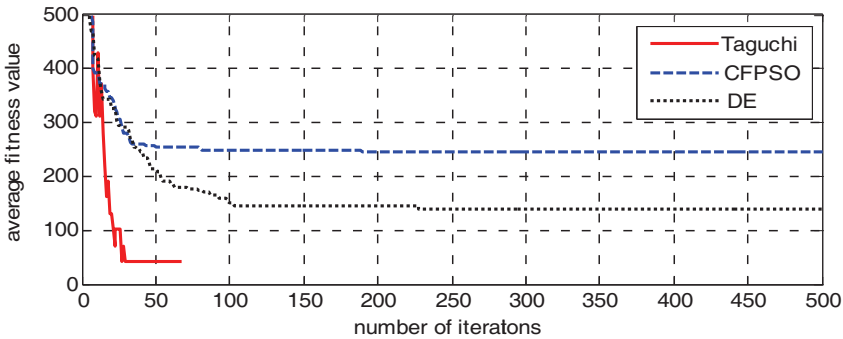


Figure 1. Comparative convergence graphs for the main-lobe-steering and null-steering beamforming problem.

the use of TagO is more suitable for the above-defined beamforming problem than the use of PSO or DE.

4.2. Main-lobe-steering and SLL-minimization Beamforming Problem

The formulation of the problem has already been given in Subsection 3.2. Again, each one of the three optimization techniques is executed 100 times in order to minimize the fitness function given in (12) and thus extract comparative convergence graphs. The techniques are applied to an 11-element ULA receiving a SOI from AoA $\theta_0 = 30^\circ$ under a low *SLL* requirement with $SLL_{des} = -30$ dB. The comparative graphs given in Figure 2 exhibit again the superiority of the TagO-based technique regarding the convergence speed, the number of iterations, and finally the ability to approach the optimal fitness value.

The better performance of the TagO-based technique can be explained by taking into account the *deterministic* nature of TagO in comparison to the *stochastic* nature of PSO and DE. In the structures of PSO and DE, a stochastic process lies behind the basic optimization procedure. This process usually helps the two methods escape from local minima but is also the main reason for increasing the number of iterations without any assurance of achieving the optimum fitness value especially in cases where the methods are eventually trapped in a local minimum. On the contrary, no stochastic process is involved in TagO. The TagO algorithm actually simulates a *full factorial strategy* by carrying out only a few experiments per iteration. Due to the optimum combination of optimization parameter values involved in each experiment, the optimum fitness value is achieved after a few iterations.

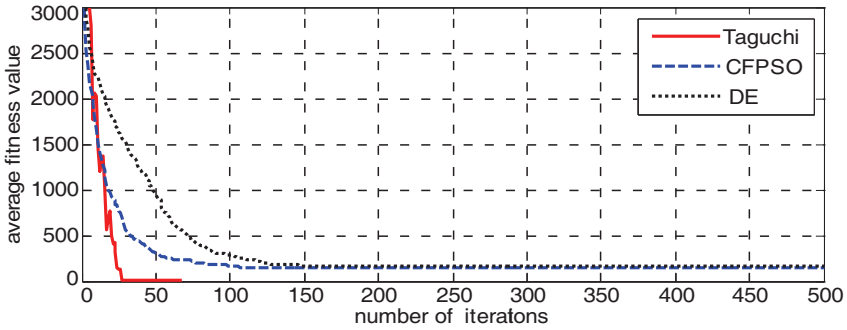


Figure 2. Comparative convergence graphs for the main-lobe-steering and SLL-minimization beamforming problem.

5. BEAMFORMING EXAMPLES

The TagO-based technique is compared here with the rest of the ABF techniques regarding its ability to solve effectively the aforementioned beamforming problems. For each one of these problems, the techniques are applied to two different sets of 1000 random cases and the results undergo a statistical analysis. Representative radiation patterns chosen respectively from the above sets are also displayed in corresponding figures. The statistical analysis and the patterns are used to evaluate the ABF techniques. The comparison is performed separately for each one of the beamforming problems.

5.1. Main-lobe-steering and Null-steering Beamforming Problem

The TagO-based, PSO-based, DE-based and SMI techniques are applied to two sets of 1000 random cases per set. The sets concern respectively five ($N = 5$) and seven ($N = 7$) interference signals. Each case is a group of $N + 1$ random AoA values $\theta_0, \theta_1, \dots, \theta_N$ different from each other. For each case, the techniques are applied to find the near-optimal weight vectors, respectively \bar{w}_{tago} , \bar{w}_{pso} , \bar{w}_{de} and \bar{w}_{smi} , that produce a main lobe towards the AoA θ_0 of the SOI and N nulls towards the AoA $\theta_1, \dots, \theta_N$ of the interference signals. Then, the radiation patterns produced respectively from \bar{w}_{tago} , \bar{w}_{pso} , \bar{w}_{de} and \bar{w}_{smi} are used to estimate the corresponding absolute angular deviations $\Delta\theta_{tago}^{main}$, $\Delta\theta_{pso}^{main}$, $\Delta\theta_{de}^{main}$ and $\Delta\theta_{smi}^{main}$ of the main lobe direction θ_0^{main} from its desired value θ_0 and the absolute angular deviations $\Delta\theta_{tago}^{null}$, $\Delta\theta_{pso}^{null}$, $\Delta\theta_{de}^{null}$ and $\Delta\theta_{smi}^{null}$ of the null directions θ_n^{null}

($n = 1, \dots, N$) from their respective desired values θ_n ($n = 1, \dots, N$). Finally, the average absolute angular deviation values $\overline{\Delta\theta}_{tago}^{\text{main}}$, $\overline{\Delta\theta}_{pso}^{\text{main}}$, $\overline{\Delta\theta}_{de}^{\text{main}}$ and $\overline{\Delta\theta}_{smi}^{\text{main}}$ concerning the main lobe direction and the average absolute angular deviation values $\overline{\Delta\theta}_{tago}^{\text{null}}$, $\overline{\Delta\theta}_{pso}^{\text{null}}$, $\overline{\Delta\theta}_{de}^{\text{null}}$ and $\overline{\Delta\theta}_{smi}^{\text{null}}$ concerning the null directions are calculated for each one of the above two sets. These values are given in Table 1 (sets 1 and 2). It seems that the TagO-based technique provides better steering ability regarding the main lobe and the nulls. The same conclusion is also derived from Figures 3 and 4, which display the optimal radiation patterns of two typical cases chosen respectively from the two sets. The radiation

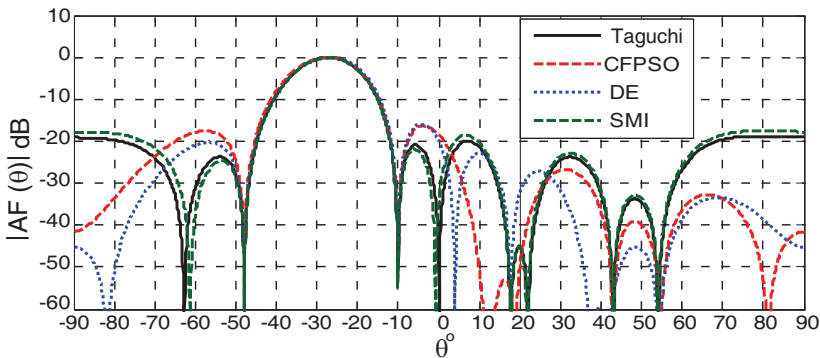


Figure 3. Optimal patterns for a desired signal arriving from $\theta_0 = -27^\circ$ and 5 interference signals arriving from AoA $-48^\circ, -10^\circ, 18^\circ, 43^\circ$ and 54° .

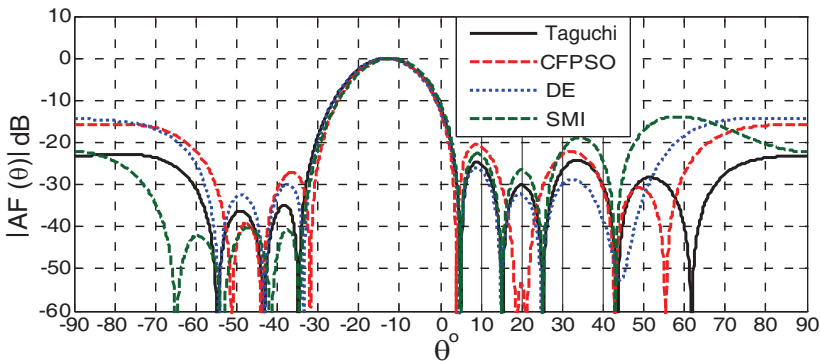


Figure 4. Optimal patterns for a desired signal arriving from $\theta_0 = -12^\circ$ and 7 interference signals arriving from AoA $-55^\circ, -44^\circ, -34^\circ, 5^\circ, 15^\circ, 25^\circ$ and 43° .

Table 1. Statistical results of the two beamforming problems.

Set	1st	2nd	Set	3rd	4th
N	5	7	SLL_{des}	-20 dB	-30 dB
$\overline{\Delta\theta}_{tago}^{main}$	0.77°	0.92°	$\overline{\Delta\theta}_{tago}^{main}$	0.27°	0.27°
$\overline{\Delta\theta}_{pso}^{main}$	0.93°	1.09°	$\overline{\Delta\theta}_{pso}^{main}$	0.31°	0.36°
$\overline{\Delta\theta}_{de}^{main}$	0.99°	1.31°	$\overline{\Delta\theta}_{de}^{main}$	0.30°	0.31°
$\overline{\Delta\theta}_{smi}^{main}$	0.80°	0.95°	$\overline{\Delta\theta}_{ml}^{main}$	0.02°	0.02°
$\overline{\Delta\theta}_{tago}^{null}$	0.23°	0.34°	\overline{SLL}_{tago}	-20.67 dB	-30.88 dB
$\overline{\Delta\theta}_{pso}^{null}$	0.26°	0.43°	\overline{SLL}_{pso}	-20.12 dB	-27.56 dB
$\overline{\Delta\theta}_{de}^{null}$	0.31°	0.62°	\overline{SLL}_{de}	-19.72 dB	-28.79 dB
$\overline{\Delta\theta}_{smi}^{null}$	0.24°	0.37°	\overline{SLL}_{ml}	-13.02 dB	-13.02 dB

Table 2. Radiation characteristics derived from Figures 3 and 4.

Figure 3	TagO	PSO	DE	SMI
$\Delta\theta^{main}$ (°)	0.10	0.20	0.50	0.50
$\overline{\Delta\theta}^{null}$ (°)	0.10	0.34	0.44	0.44
$SINR$ (dB)	19.17	18.87	18.67	18.67
Average null depth (dB)	-62.08	-58.35	-55.25	-55.24
Figure 4	TagO	PSO	DE	SMI
$\Delta\theta^{main}$ (°)	0.70	0.90	1.30	0.20
$\overline{\Delta\theta}^{null}$ (°)	0.29	1.30	0.49	0.29
$SINR$ (dB)	19.02	17.50	18.52	18.81
Average null depth (dB)	-60.17	-43.52	-53.59	-56.93

characteristics concerning the patterns of the two figures are given in Table 2.

5.2. Main-lobe-steering and SLL-minimization Beamforming Problem

The TagO-based, PSO-based, DE-based and ML techniques are applied to two new sets of 1000 random cases per set. Each set corresponds to a different value of SLL_{des} . This value is considered equal to -20 dB and -30 dB respectively for the two sets. Each case

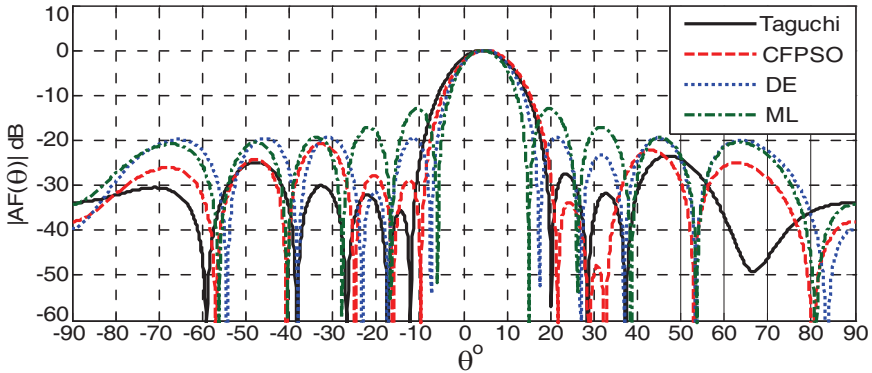


Figure 5. Optimal patterns for $\theta_0 = 4.5^\circ$ and $SLL_{des} = -20$ dB.

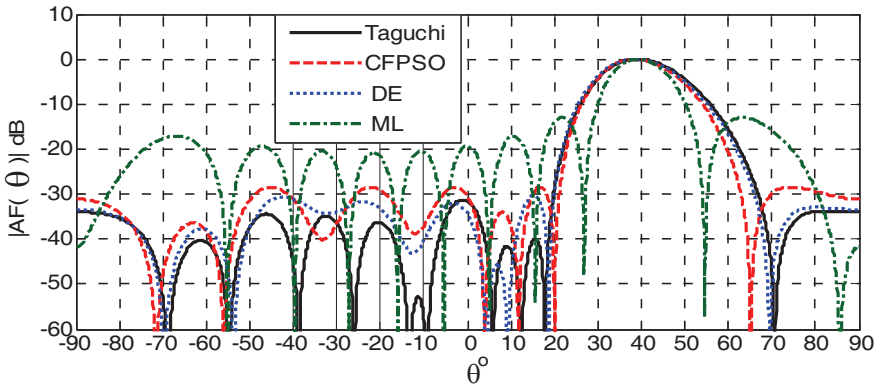


Figure 6. Optimal patterns for $\theta_0 = 39.5^\circ$ and $SLL_{des} = -30$ dB.

corresponds to a random value of θ_0 . For each case, the techniques are applied to find the near-optimal weight vectors, respectively \bar{w}_{tago} , \bar{w}_{pso} , \bar{w}_{de} and \bar{w}_{ml} , that produce a main lobe towards θ_0 and minimize the SLL below SLL_{des} . The radiation patterns produced respectively from \bar{w}_{tago} , \bar{w}_{pso} , \bar{w}_{de} and \bar{w}_{ml} are used to estimate the corresponding absolute angular deviations $\Delta\theta_{tago}^{main}$, $\Delta\theta_{pso}^{main}$, $\Delta\theta_{de}^{main}$ and $\Delta\theta_{ml}^{main}$ of the main lobe direction θ_0^{main} from its desired value θ_0 and the corresponding side lobe levels SLL_{tago} , SLL_{pso} , SLL_{de} and SLL_{ml} . Finally, the average values $\overline{\Delta\theta}_{tago}^{main}$, $\overline{\Delta\theta}_{pso}^{main}$, $\overline{\Delta\theta}_{de}^{main}$, $\overline{\Delta\theta}_{ml}^{main}$, \overline{SLL}_{tago} , \overline{SLL}_{pso} , \overline{SLL}_{de} and \overline{SLL}_{ml} are calculated for each set. These values are given in Table 1 (sets 3 and 4). Also, two typical cases are chosen

Table 3. Radiation characteristics derived from Figures 5 and 6.

Figure 5	TagO	PSO	DE	ML
$\Delta\theta^{\text{main}}$ ($^{\circ}$)	0.10	0.70	0.50	0.03
SLL (dB)	-23.43	-20.77	-19.28	-13.02
Figure 6	TagO	PSO	DE	ML
$\Delta\theta^{\text{main}}$ ($^{\circ}$)	0.20	0.60	0.60	0.02
SLL (dB)	-31.34	-28.39	-30.34	-13.02

respectively from the two sets in order to display the corresponding optimal patterns (Figures 5 and 6). By taking into account the results of Table 1, the optimal patterns of Figures 5 and 6, and the radiation characteristics of these patterns given in Table 3, it seems that the TagO-based technique outperforms the other techniques regarding both the main lobe steering and the SLL minimization.

6. CONCLUSION

A new ABF technique based on Taguchi's Optimization method has been presented. Modifications have been proposed to improve the applicability of the method and save computational time. The technique is applied to solve two different beamforming problems by using a suitably chosen fitness function for each problem. The main lobe steering is a common requirement for both problems. The null steering and the SLL minimization below a desired SLL value are two additional requirements respectively for the two problems.

The TagO-based ABF technique was compared in terms of convergence with two other techniques based respectively on PSO and DE. The comparison was applied to both beamforming problems and revealed the superiority of the TagO-based technique regarding its high convergence speed in combination with its ability to achieve better fitness values in less time than the other two techniques. Therefore, the TagO algorithm is more suitable for real time applications, such as ABF, than other optimization algorithms.

A statistical analysis was performed on the ABF results of both beamforming problems and showed that the TagO-based technique outperforms several ABF techniques regarding the aforementioned requirements of the problems. Consequently, the TagO method seems to be promising in smart antenna applications.

REFERENCES

1. Caorsi, S., M. Donelli, A. Lommi, and A. Massa, "A real-time approach to array control based on a learned genetic algorithm," *Microwave and Optical Technology Letters*, Vol. 36, 235–238, 2003.
2. Donelli, M., A. Lommi, A. Massa, and C. Sacchi, "Assessment of the GA-based adaptive array control strategy: The case of stochastic life-time co-channel interferences," *Microwave and Optical Technology Letters*, Vol. 37, 198–201, 2003.
3. Sacchi, C., F. De Natale, M. Donelli, A. Lommi, and A. Massa, "Adaptive antenna array control in the presence of interfering signals with stochastic arrivals: Assessment of a GA-based procedure," *IEEE Transactions on Wireless Communications*, Vol. 3, No. 4, 1031–1036, Jul. 2004.
4. Donelli, M., R. Azaro, F. G. B. De Natale, and A. Massa, "An innovative computational approach based on a particle swarm strategy for adaptive phased-arrays control," *IEEE Transactions on Antennas and Propagation*, Vol. 54, No. 3, 888–898, Mar. 2006.
5. Benedetti, M., R. Azaro, D. Franceschini, and A. Massa, "PSO-based real-time control of planar uniform circular arrays," *IEEE Antennas and Wireless Propagation Letters*, Vol. 5, No. 1, 545–548, Dec. 2006.
6. Benedetti, M., R. Azaro, and A. Massa, "Memory enhanced PSO-based optimization approach for smart antennas control in complex interference scenarios," *IEEE Transactions on Antennas and Propagation*, Vol. 56, No. 7, 1939–1947, Jul. 2008.
7. Benedetti, M., R. Azaro, and A. Massa, "Experimental validation of a fully-adaptive smart antenna prototype," *Electronics Letters*, Vol. 44, No. 11, 661–662, 2008.
8. Benedetti, M., G. Oliveri, P. Rocca, and A. Massa, "A fully-adaptive smart antenna prototype: Ideal model and experimental validation in complex interference scenarios," *Progress In Electromagnetics Research*, Vol. 96, 173–191, 2009.
9. Viani, F., L. Lizzi, M. Donelli, D. Pregnotato, G. Oliveri, and A. Massa, "Exploitation of parasitic smart antennas in wireless sensor networks," *Journal of Electromagnetic Waves and Applications*, Vol. 24, No. 7, 993–1003, 2010.
10. Umrani, A. W., Y. Guan, and F. A. Umrani, "Effect of steering error vector and angular power distributions on beamforming and transmit diversity systems in correlated fading channel," *Progress In Electromagnetics Research*, Vol. 105, 383–402, 2010.
11. Poli, L., P. Rocca, G. Oliveri, and A. Massa, "Adaptive nulling in

- time-modulated linear arrays with minimum power losses,” *IET Microwaves, Antennas & Propagation*, Vol. 5, No. 2, 157–166, 2011.
12. Lee, J.-H., Y.-S. Jeong, S.-W. Cho, W.-Y. Yeo, and K. S. J. Pister, “Application of the newton method to improve the accuracy of toa estimation with the beamforming algorithm and the music algorithm,” *Progress In Electromagnetics Research*, Vol. 116, 475–515, 2011.
 13. Zaharis, Z. D. and T. V. Yioultis, “A novel adaptive beamforming technique applied on linear antenna arrays using adaptive mutated boolean PSO,” *Progress In Electromagnetics Research*, Vol. 117, 165–179, 2011.
 14. Mallipeddi, R., J. P. Lie, P. N. Suganthan, S. G. Razul, and C. M. S. See, “A differential evolution approach for robust adaptive beamforming based on joint estimation of look direction and array geometry,” *Progress In Electromagnetics Research*, Vol. 119, 381–394, 2011.
 15. Mallipeddi, R., J. P. Lie, P. N. Suganthan, S. G. Razul, and C. M. S. See, “Near optimal robust adaptive beamforming approach based on evolutionary algorithm,” *Progress In Electromagnetics Research B*, Vol. 29, 157–174, 2011.
 16. Lee, J.-H., G.-W. Jung, and W.-C. Tsai, “Antenna array beamforming in the presence of spatial information uncertainties,” *Progress In Electromagnetics Research B*, Vol. 31, 139–156, 2011.
 17. Lee, J.-H., “Robust antenna array beamforming under cycle frequency mismatch,” *Progress In Electromagnetics Research B*, Vol. 35, 307–328, 2011.
 18. Jabbar, A. N., “A novel ultra-fast ultra-simple adaptive blind beamforming algorithm for smart antenna arrays,” *Progress In Electromagnetics Research B*, Vol. 35, 329–348, 2011.
 19. Mallipeddi, R., J. P. Lie, S. G. Razul, P. N. Suganthan, and C. M. S. See, “Robust adaptive beamforming based on covariance matrix reconstruction for look direction mismatch,” *Progress In Electromagnetics Research Letters*, Vol. 25, 37–46, 2011.
 20. Gross, F. B., *Smart Antennas for Wireless Communications with Matlab*, McGraw-Hill, New York, 2005.
 21. Weng, W. C., F. Yang, and A. Elsherbini, *Electromagnetics and Antenna Optimization Using Taguchi’s Method*, Morgan & Claypool, San Rafael, CA, 2007.
 22. Weng, W. C. and C. Choi, “Optimal design of CPW slot antennas using Taguchi’s method,” *IEEE Trans. on Magnetics*, Vol. 45,

- No. 3, 1542–1545, Mar. 2009.
23. Dib, N. I., S. K. Goudos, and H. Muhsen, “Application of Taguchi’s optimization method and self-adaptive differential evolution to the synthesis of linear antenna arrays,” *Progress In Electromagnetics Research*, Vol. 102, 159–180, 2010.
 24. Sheng, N., C. Liao, W. Lin, L. Chang, Q. Zhang, and H. Zhou, “A hybrid optimized algorithm based on EGO and Taguchi’s method for solving expensive evaluation problems of antenna design,” *Progress In Electromagnetics Research C*, Vol. 17, 181–192, 2010.
 25. Nemri, N., A. Smida, R. Ghayoula, H. Trabelsi, and A. Gharsallah, “Phase-only array beam control using a Taguchi optimization method,” *11th Mediterranean Microwave Symposium (MMS)*, 97–100, Sept. 2011.
 26. Eberhart, R. C. and Y. Shi, “Particle swarm optimization: Developments, applications and resources,” *Proceedings of the Congress on Evolutionary Computation*, Vol. 1, 81–86, 2001.
 27. Lizzi, L. and G. Oliveri, “Hybrid design of a fractal-shaped GSM/UMTS antenna,” *Journal of Electromagnetic Waves and Applications*, Vol. 24, Nos. 5–6, 707–719, 2010.
 28. Wang, J., B. Yang, S. H. Wu, and J. S. Chen, “A novel binary particle swarm optimization with feedback for synthesizing thinned planar arrays,” *Journal of Electromagnetic Waves and Applications*, Vol. 25, Nos. 14–15, 1985–1998, 2011.
 29. Wang, W.-B., Q. Feng, and D. Liu, “Application of chaotic particle swarm optimization algorithm to pattern synthesis of antenna arrays,” *Progress In Electromagnetics Research*, Vol. 115, 173–189, 2011.
 30. Li, W.-T., Y.-Q. Hei, and X.-W. Shi, “Pattern synthesis of conformal arrays by a modified particle swarm optimization,” *Progress In Electromagnetics Research*, Vol. 117, 237–252, 2011.
 31. Liu, D., Q. Feng, W.-B. Wang, and X. Yu, “Synthesis of unequally spaced antenna arrays by using inheritance learning particle swarm optimization,” *Progress In Electromagnetics Research*, Vol. 118, 205–221, 2011.
 32. Goudos, S. K., K. Siakavara, E. Vafiadis, and J. N. Sahalos, “Pareto optimal yagi-uda antenna design using multi-objective differential evolution,” *Progress In Electromagnetics Research*, Vol. 105, 231–251, 2010.
 33. Goudos, S. K., Z. D. Zaharis, and T. V. Yioultis, “Application of a differential evolution algorithm with strategy adaptation to the design of multi-band microwave filters for wireless communica-

- tions,” *Progress In Electromagnetics Research*, Vol. 109, 123–137, 2010.
34. Li, R., L. Xu, X.-W. Shi, N. Zhang, and Z.-Q. Lv, “Improved differential evolution strategy for antenna array pattern synthesis problems,” *Progress In Electromagnetics Research*, Vol. 113, 429–441, 2011.
 35. Yang, P., F. Yang, and Z.-P. Nie, “DOA estimation with sub-array divided technique and interpolated esprit algorithm on a cylindrical conformal array antenna,” *Progress In Electromagnetics Research*, Vol. 103, 201–216, 2010.
 36. Park, G. M., H. G. Lee, and S. Y. Hong, “DOA resolution enhancement of coherent signals via spatial averaging of virtually expanded arrays,” *Journal of Electromagnetic Waves and Applications*, Vol. 24, No. 1, 61–70, 2010.
 37. Lui, H. S. and H. T. Hui, “Effective mutual coupling compensation for direction-of-arrival estimations using a new, accurate determination method for the receiving mutual impedance,” *Journal of Electromagnetic Waves and Applications*, Vol. 24, Nos. 2–3, 271–281, 2010.
 38. Li, R., L. Xu, X. -W. Shi, L. Chen, and C. -Y. Cui, “Two-dimensional NC-Music DOA estimation algorithm with a conformal cylindrical antenna array,” *Journal of Electromagnetic Waves and Applications*, Vol. 25, Nos. 5–6, 805–818, 2011.
 39. Liang, J. and D. Liu, “Two l-shaped array-based 2-d DOAs estimation in the presence of mutual coupling,” *Progress In Electromagnetics Research*, Vol. 112, 273–298, 2011.
 40. Kim, Y. and H. Ling, “Direction of arrival estimation of humans with a small sensor array using an artificial neural network,” *Progress In Electromagnetics Research B*, Vol. 27, 127–149, 2011.